Neuronal oscillations predict un-cued task switching in the Wisconsin card sorting test

Judith Sattelberger[1,2*], Hamed Haque[1], Mengxing Liu[3], Jaana Simola[4], J Matias Palva[1,5], Michael M. Halassa[3], Satu Palva[1,6*]

[1] Neuroscience Center, Helsinki Institute of Life Science, University of Helsinki, FI-00014 Helsinki, Finland

[2] BioMag Laboratory, HUS Medical Imaging Centre, Helsinki University Central Hospital, FI-00029 HUS, Finland

[3] Department of Neuroscience, Tufts University School of Medicine, Boston, MA 02111, USA

[4] Faculty of Educational Sciences, University of Helsinki, FI-00140 Helsinki, Finland

[5] Department of Neuroscience and Bioengineering (NBE), Aalto University, FI-02150 Espoo, Finland

[6] School of Psychology and Neuroscience, University of Glasgow, G12 8QB Glasgow, UK

*Correspondence should be addressed to Judith Sattelberger (judith.sattelberger@helsinki.fi) or Satu Palva (satu.palva@helsinki.fi)

Running Title: Oscillations underlie task switching in the WCST

Funding: This work was supported by the Sigrid-Juselius-Foundation (grant number 240156 to SP/JMP).

CRediT author contribution(s):

JuS: Conceptualization, Data curation, Formal analysis, Investigation, Methodology, Project administration, Software, Visualization, Writing –original draft, HH: Conceptualization, Methodology, ML: Formal analysis, Methodology, JaS: Data curation, Investigation, Software, JMP: Conceptualization, Funding acquisition, Methodology, Resources, Writing – review & editing, MMH: Conceptualization, Methodology, Writing – Review & Editing, SP: Conceptualization, Funding acquisition, Methodology, Project administration, Supervision, Visualization, Writing – original draft, Writing – review & editing

Conflict of interest statement: The authors declare no competing financial interests.

Acknowledgements: The authors would like to thank Jasmin Elonen for preprocessing the MEG data.

Abstract

Cognitive flexibility is the fundamental ability to rapidly adapt behavior to the environment, even when the contextual rules are implicit and change suddenly. Such type of task switching is commonly measured with the Wisconsin Card Sorting Test (WCST), in which cards need to be sorted by a changing rule that is not explicit to participants and thus needs to be deduced from feedback. Crucially, this ability to adapt to changing task rules in the absence of instructive cues shows large individual variability of which neural mechanisms have remained unknown. Preparative un-cued task switching has previously been connected to prefrontal theta and parietal alpha band amplitude modulations. However, it has remained unknown whether these local oscillation dynamics or large-scale network interactions would enable cognitive flexibility and explain the interindividual performance differences therein. Here, to test this possibility, we collected MEG data during the WCST from N = 26 participants. To assess individual variability in cognitive flexibility, we calculated the number of late errors as a proxy for learning speed and implemented a new sequential learning model for estimating the impact of feedback sensitivity on individual performance. To investigate the neural dynamics, we computed local and network oscillation dynamics from individually source-reconstructed data. Higher switching accuracy was predicted by local gamma (52–96 Hz) band amplitude increases and parietal alpha (7–13 Hz) and beta (13–32 Hz) band suppression as well as sustained frontoparietal alpha band (9–15 Hz) network desynchronization. Individuals with higher sensitivity to positive feedback showed larger alpha- and beta-band amplitude modulations and alpha network desynchronization, whereas sensitivity to negative feedback was mainly associated with larger gamma amplitudes. Our results demonstrate that individual variability in un-cued task switching is due to differential learning speed and sensitivity to feedback, the neural basis of which relies on distinct local and large-scale oscillatory network mechanisms.

Keywords: cognitive control, oscillations, task switching, synchrony, WCST

Introduction

Cognitive flexibility is a key component of cognitive control alongside top-down attention and inhibition, enabling us to quickly adapt behavior to an unpredictable and changing environment. This executive function varies widely between individuals and over the lifetime (Guarino et al., 2020; Kupis et al., 2021; Peltz et al., 2011). The ability to adapt to changing task rules, even when they are not explicitly instructed, but need to be inferred from feedback, is called un-cued task switching. Un-cued task switching has often been studied with the Wisconsin Card Sorting Test (WCST) in humans (Berg, 1948; Miles et al., 2021), monkeys (Kuwabara et al., 2014; Mansouri et al., 2006; Roberts et al., 1994) and recurrent neural networks in computational work (Liu and Wang, 2024; Zheng et al., 2024). During this task, a card with multiple features needs to be sorted to the matching target card based on the relevant feature dimension (i.e. the task rule), which changes across trials. Importantly, the task rule needs to be inferred from feedback and is not explicitly instructed. As evidenced by functional magnetic resonance imaging (fMRI) data, WCST performance depends critically on activation of the prefrontal cortex (PFC) (Buckley et al., 2009; Sakai, 2008), in line with the PFC's general role in cognitive control tasks (Bissonette et al., 2013; Panikratova et al., 2020; Ravizza & Ciranni, 2002; Robbins et al., 1996; Tsuchida & Fellows, 2013).

Brain rhythms – neuronal oscillations – are fundamental for temporal coordination of neuronal processing both locally within brain areas as well as across regions (Fries, 2015; Palva and Palva, 2012; Singer, 1999). Traditionally, oscillatory and other brain systems-level mechanisms of task switching have been studied with electroencephalography (EEG) and cued paradigms that inform about an upcoming task change and instruct on the required behavior. These studies have revealed modulations of oscillations in multiple frequency bands across multiple cortical areas (G. Gratton et al., 2018). Typically, theta (θ, 3–8 Hz) band oscillations in the PFC or the midline θ activity are thought to play a pivotal role in cognitive control (see Cavanagh et al., 2009; Cavanagh & Frank, 2014; Cohen, 2011; Cohen et al., 2007; Sauseng et al., 2010) including conflict monitoring (Cohen & Cavanagh, 2011; Riddle et al., 2020; Sauseng & Liesefeld, 2020) as well as proactive or anticipatory control dynamics needed for un-cued task switching (Cooper et al., 2015; Cooper et al., 2017; Cunillera et al., 2012; Sauseng et al., 2006). In addition to θ activity, there is also some evidence for the role of gamma (γ, 30–100 Hz) (Proskovec et al., 2019), parietal alpha (α, 8–12 Hz) (Foxe et al., 2014; Murphy et al., 2016; Verstraeten & Cluydts, 2002), and beta band (β, 13–30 Hz) (Cunillera et

al., 2012; Gladwin et al., 2006) amplitudes in enhancing cued task-switching performance, with the α-band oscillations over sensory areas putatively facilitating top-down selection of task-relevant features (Keitel et al., 2019; Kaiser et al., 2023) and initiating the behavioral switch (Mansfield et al., 2012; Foxe et al., 2014; Cunillera et al., 2012; Foxe et al., 2014; Gladwin et al., 2006; Murphy et al., 2016; Proskovec et al., 2019; Verstraeten & Cluydts, 2002). However, as the majority of previous studies on task switching have been based on local EEG sensor level data, there being limited understanding of the cortical sources of these effects, the functional role of oscillations have remained debated (Brass et al., 2005; van Driel et al., 2012). Importantly, it is further not known whether these mechanisms are also relevant for un-cued task switching that depends on the internal ability to switch rules based on behavior demands and feedback.

Multimodal network research across species indicates that long-range connections between cortical areas are crucial for cognitive flexibility. Research in non-human primates has evidenced that the mediodorsal thalamus and its interactions with the PFC are key to enable cognitive flexibility (Rikhye et al., 2018; Wolff and Halassa, 2024), especially under task uncertainty (Huang et al., 2024; Zhang et al., 2025). However, there are almost no studies on long-range oscillatory coupling in relation to cognitive control or task switching in humans that apply electrophysiological methods that yield rich local field potential data comparable to animal models such as magnetoencephalography (MEG) (Baillet, 2017; Hari and Salmelin, 1997). However related, MEG studies using source connectivity analysis with precise anatomical mapping have found evidence that long-range α band phase synchronization between the PFC and sensory regions supports top-down attentional selection (Lobier et al., 2018; D'Andrea et al., 2019) and explain individual performance variability in visual working memory (VWM) performance (Palva et al., 2010; Ericson et al., 2024; Sattelberger et al., 2024). The cross-frequency interactions of θ/α band oscillations with higher frequencies of β/γ oscillations via phase-amplitude coupling (PAC) and phase-synchrony has further been shown to predict performance in VWM (Biel et al., 2021; Bahramisharif et al., 2018; Brooks et al., 2020; Lisman & Jensen, 2013; Peylo et al., 2022; Siebenhühner et al., 2016), attention (Cansler et al., 2023; Esghaei et al., 2022; Papaioannou et al., 2022) and a conflict-processing task (Chen et al., 2022). Similarly to long-range oscillatory networks there is no evidence for their relevance in cognitive flexibility.

Despite the likelihood that dynamic oscillatory network fluctuations would be fundamental for enabling internally guided switching of cognitive rules or tasks, this has remained uncharted. Critically, prior studies on neuronal mechanisms of task switching have largely used externally cued task switching paradigms. Importantly, while the correct task rule following each cue is known to the participant in a cued task-switching paradigm, necessitating only a behavioral switch (for an overview, see Kiesel et al., 2010), in the un-cued WCST, the participant needs to integrate concurrent error monitoring of every response with preparative switching during the planning period to deduct the new correct rule out of all possible rules (Barcelo, 2003; Martin, 2006). While this requires a fast and accurate response to both positive and negative feedback, only few studies have investigated the neural basis of inter-individual differences in feedback sensitivity on task behavior (Bishara et al., 2010). To investigate whether internally driven un-cued task switching and the individual performance therein would depend on concurrent modulations of local oscillations and large-scale oscillatory networks, we collected MEG data of participants completing the WCST task. We then identified changes in local oscillation amplitudes and phase-synchronized networks from their source-reconstructed cortical activity during the planning period of the task where error monitoring, inhibition of alternative rules and preparative switching take place. Importantly, we identified how these neuronal dynamics could be explained by differences in feedback sensitivity by applying a sequential learning model.

Methods and Materials

Participants and experimental design

Twenty-six healthy adults (mean age 33.2 (SD 10.2), age range 18–57 years, 11 females) participated in the study. All participants reported normal or corrected-to-normal vision, no recent history of neuropsychological or neurological illness, and physical eligibility to undergo MEG and MRI measurements. The study was approved by the Helsinki University Hospital ethical committee and was carried out according to the Declaration of Helsinki. All participants provided written informed consent before the experiment. Participants completed the Wisconsin card sorting test (WCST, Fig. 1A) by Grant and Berg (1948), adapted as a computerized version by Barcelo (Barcelo, 2003) with the Presentation™ software

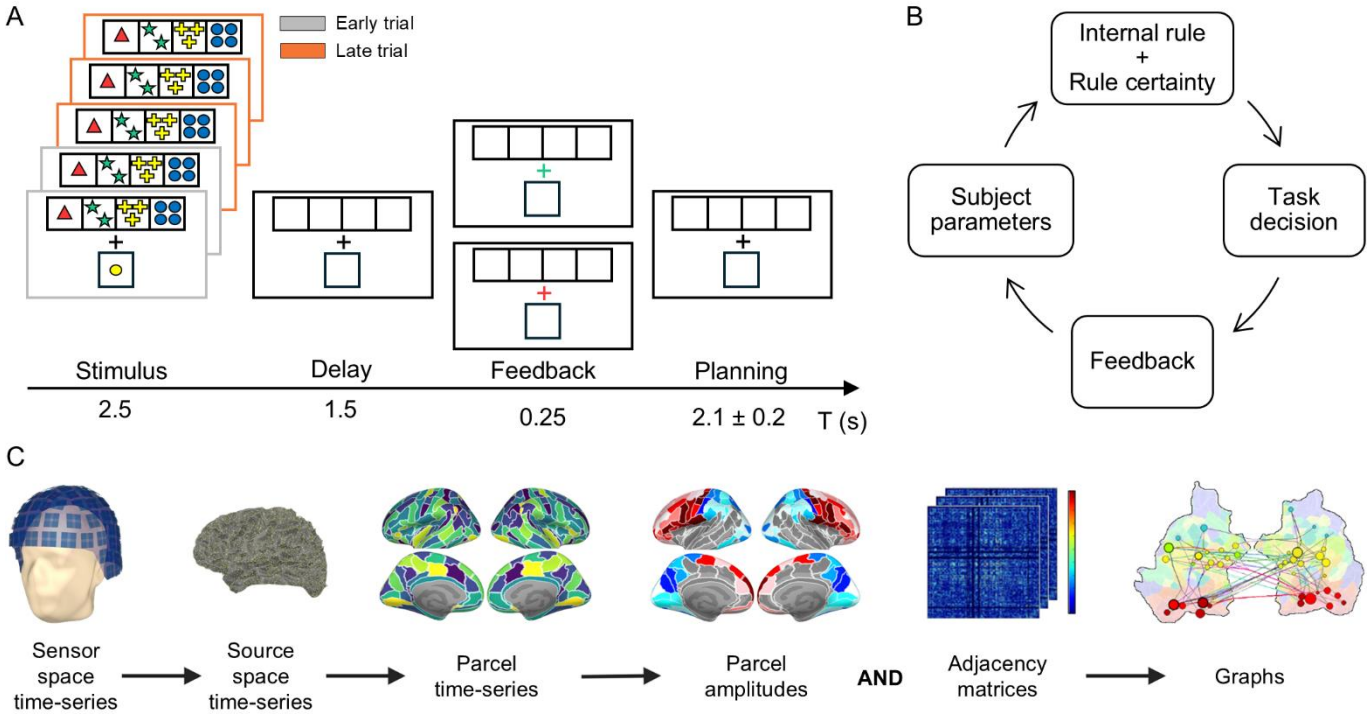

Figure 1. Experimental paradigm. A. Schematic of one trial series of the Wisconsin card sorting test. In each trial, a sample card (bottom row) and four target cards (top row) were shown and the participant sorted the sample card to one of the target cards. A green or red feedback cross was shown after the response to indicate a correct or incorrect response, respectively. **B**. Schematic of the behavioral modelling. In the beginning of each trial, the participant had an internal rule for the current series. Based on this rule, the participant made a task decision to sort the card to one of the three categories, leading to positive or negative feedback. Depending on the subject's individual tendency to respond to feedback as measured by the subject parameters, this feedback modified the internal rule and increased the certainty of that rule. **C.** Schematic of the MEG analysis. Cortical sources were reconstructed from broad-band MEG time-series data, collapsed into 200 cortical parcels of the Destrieux atlas and used for estimating oscillation amplitudes and phase-synchronization between parcels.

(Neurobehavioral Systems, Inc., Albany, CA, USA). Here, the participants needed to sort cards according to three rule-categories: shape (circle, star, cross, or triangle), color (blue, yellow, red, or green), or number of items (one to four). The category by which to sort changed on every fifth trial and needed to be deduced by the participant through trial and error based on feedback. Participants were not informed how often the rule would change or what the next correct sorting category would be. In each trial, a sample card (bottom

row), a white fixation cross, and four target cards (top row) were shown for 2.5 s before a light grey background. This was followed by a 1.5 s delay, during which the participant could sort the stimulus card to one of the target cards, depending on the currently active rule (same number, color, or shape). A green or red feedback cross was shown for 0.25 s after the response to indicate a correct or incorrect response, respectively, followed by the planning stage lasting 1.9 to 2.3 s.

The stimulus card was a rectangle of 7.3 x 5.5 deg, and the target cards were rectangles of 4.2 x 3.0 deg visual angle. A black fixation cross (0.65 x 0.48 deg) and black outlines of the stimulus and target cards (same sizes as the cards) were present throughout the whole trial in the center of this stimulus window. The target cards remained the same for the entire experiment. The sample card was selected randomly from 24 unambiguous cards of the original 64 WCST cards (Perianez et al., 2004; Barcelo et al., 2002), meaning that only one target card fit the current rule category. The rule orders were selected pseudo-randomly so that the same rule was not immediately repeated. The experiment consisted of three blocks with 150 trials, where one block had an average duration of 15 minutes and participants could rest between them.

Statistical analysis of behavioral data

After removal of trials without response (4 % of all trials), RTs were calculated as the duration from stimulus onset to response separately for trials following negative feedback (RTshift) and those following positive feedback (RTstay). Hit rates (HRs) were then calculated as the proportion of correct responses from all trials. We also categorized incorrect responses during the first two trials of a rule series as early errors and all subsequent errors as late errors, allowing us to assess the learning speed of participants. We then computed HRs for every trial in a rule series separately to confirm that the mean performance during early trials was at chance level and exceeded thereafter. Next, we compared subjects' mean RTshift and RTstay with a two-tailed t-test for paired samples and subsequently checked if RTshift and RTstay were correlated with the number of late errors (NLE) across subjects using the Pearson correlation coefficient. Additionally, we tested whether differences in NLE, RTshift, and RTstay covaried with age (Pearson correlation coefficient) or sex (independent samples t-test).

In addition to this behavioral analysis, we developed a sequential learning model to capture the effect of positive and negative feedback on task behavior (Fig. 1B) based on the model by Bishara and colleagues (2010). Here, we estimated the subject-wise parameters r (reward sensitivity), p (punishment sensitivity), e (exploration tendency), and a (anticipation tendency) across trials. While r and p are equivalent to Bishara et al. (2010), we added e to assess the effect of rule shifting despite preceding positive feedback and a as the subjects' ability to predict an upcoming rule change after 5 trials. We then used multiple linear regressions to check if these parameters could explain behavioral performance measures. Lastly, we also estimated the trial-to-trial rule certainty by creating an attention weight vector that represents the participant's chosen rule in the previous trial (see Bishara et al. 2010). Each value in this vector represents the probability of the active rule being shape, number, or color (e.g., [0,0,1] if the rule is known to be color). This vector is updated on every trial based on the card choice of the participant and the resulting feedback. Consequently, the rule uncertainty of one trial is first calculated as the Jensen-Shannon distance between the attention weight vectors of current trial and one trial before, being largest after a rule shift and becoming smaller after receiving positive feedbacks, from which we then obtain the rule certainty by inversion (rule certainty = 1 - rule uncertainty).

MEG and MRI recordings, preprocessing and filtering

Participants sat approximately 130 cm from the projector screen (VPixx; resolution: 1920 × 1080 pixels; refresh rate: 120 Hz). Stimuli were presented with the Presentation™ software (Neurobehavioral Systems, Inc., Albany, CA, USA). A photodiode was used to achieve ± 1 ms precision of stimulus presentation. We recorded MEG with 204 planar gradiometers and 102 magnetometers with a Triux (Elekta Neuromag Ltd.) system at 1000 Hz sampling rate and an online band-pass filter of 0.03–330 Hz at the BioMag Laboratory in the Helsinki University Hospital. Ocular artifacts were measured with electro-oculogram (EOG) electrodes. Participants' responses were recorded with a hand-held fiber-optic response device and responded to finger lifts.

In addition, whole head magnetic resonance images (MRIs; Siemens Verio 1.5 T) were taken from all subjects for the source-reconstruction of MEG data with the magnetization-prepared rapid acquisition

gradient echo (MPRAGE) sequence at a resolution of 1 mm voxel size. Maxfilter software (Elekta Neuromag) was used for temporal signal space separation (tSSS) to suppress extra-cranial noise in MEG data, to adjust for head position changes during the measurements, and to interpolate bad channels (Taulu & Kajola, 2005; Taulu & Simola, 2006). Head position changes over 10 mm were excluded from the raw data and raw MEG data was then notch-filtered at 50 Hz and harmonics. Independent component analysis (MATLAB) was used for identifying and extracting ocular and heartbeat artefacts. The MEG data was then frequency-filtered using 38 approximately logarithmically spaced Morlet wavelets from 3 to 143 Hz with 5 cycles.

Source modelling

In order to obtain precise source localization of MEG signals optimized for every participant's individual brain anatomy, we applied a multistep source modelling approach (Fig. 1C).The open-access software Freesurfer (http://surfer.nmr.mgh.harvard.edu) was used for volumetric segmentation of the MRI data, surface reconstruction, flattening, and cortical parcellation/labeling with the Destrieux atlas (Destrieux, Fischl, Dale & Halgren, 2010). The software MNE-Python (Gramfort et al. 2013) was used for MEG-MRI colocalization, and preparation of the forward and inverse operators. For every subject, we created the source space with dipole orientations fixed to the pial surface normals and a 5 mm inter-dipole separation, a 1-layer boundary element method (BEM) model from the inner skull, and the BEM solution. Noise-covariance matrices (NCMs) were computed with a regularization constant of 0.05 using narrowband 151–299 Hz filtered resting-state data (1 min) to compute a forward solution and the inverse operator that transform the filtered complex single-trial MEG time series to source-vertex time series. Source-space vertices were then collapsed into 400 cortical parcels using fidelity optimized collapse operators (Korhonen et al, 2014), assigning each parcel to one of 7 functional networks (Yeo et al. 2011) before morphing them into 200 larger parcels to increase statistical power. We epoched data into trial sequences of 2.65 s length and rejected trials with blinks during the feedback.

Analysis of oscillation amplitudes and inter-areal phase synchrony

To analyze the effect of set-switching on oscillation amplitudes and inter-areal phase synchrony, we separated trials into two conditions: shift trials (previous trial's feedback was negative) and stay trials (previous trial's feedback was positive). We computed the amplitude envelope for each condition, subject, wavelet frequency, and parcel across all trials and samples. Then, we applied baseline-correction (0.5–0 s prior S1 onset) through baseline subtraction. To obtain time-averaged oscillation amplitudes for statistical comparisons, we constructed a sliding time window of 100 ms length that was moved along the time axis with 50 ms distance to the start of the previous window, creating an overlap of 50 ms, separately for every frequency. The absolute values of all samples within the sliding time window were then averaged.

To identify robust cortex-wide phase-synchrony networks, we first averaged the complex signal across trials for each condition and subject, excluding 3 subjects with a small number of shift trials ($N < 60$). We then computed the imaginary part of the phase locking value (iPLV) between each parcel-parcel pair with a sliding time window of 400 ms length, 100 ms distance, and 300 ms overlap. The first time window (0.4–0 s prior S1 onset) served as the baseline for phase synchrony analysis through baseline subtraction.

Statistical analysis of neuronal data

To estimate the robustness of oscillation amplitude modulations and changes in inter-areal phase synchronization across the whole cortex, we calculated the fraction of cortical parcels with a significant effect out of all 200 parcels (P+/P-) and the connection density (K+/K-), that is the fraction of significant parcel-parcel connections out of all connections. A two-sided Wilcoxon-signed rank test was used for testing statistical differences between shift and stay conditions and the baseline as well as their contrast shift-stay for oscillation amplitudes and inter-areal phase synchronization. Significant amplitude and phase synchrony changes across the course of a rule series were obtained by computing Spearman's r. We also calculated Spearman's r to assess the correlation of behavioral performance measures with the mean amplitude and mean phase synchronization of each subject. To estimate effect sizes, we selected time-frequency (TF) windows of interest showing the most robust (largest P+/P- values for amplitude and K+/K- for phase synchronization) differences between shift and stay conditions and calculated the average difference

between all parcels/edges as $r = Z \sqrt{N}$ (Rosenthal, 1991). All statistical comparisons were corrected for multiple comparisons by rejecting a percentage of the highest p values in each TF bin corresponding to the used alpha level of significant parcels (i.e., we rejected the highest 5 % if alpha level was 0.05). Additionally, we controlled for multiple comparisons by applying a threshold q to those significant results that are expected to arise by chance given the number of hypothesis tests and alpha level and indicated the q threshold together with the alpha level in the figure legends. We only visualized oscillation amplitude modulations and inter-areal synchronization changes that exceeded the q-threshold across frequencies in time-frequency representations (TFRs).

To estimate n:m phase amplitude coupling (PAC), we compared the phase of all low frequencies (3–8 Hz) to the phase of the amplitude envelope of high frequencies (9–143 Hz) by computing the PLV between all edge pairs. This was done for each subject and for the averaged trials of conditions shift and stay separately in the time window 0.6 to 1.6 s after feedback onset. Because PLV is sensitive to the number of trials, we equalized the number of trials between conditions to the lowest number within each subject before averaging, again excluding 3 subjects with $N < 60$ shift trials. We then estimated the statistical significance across the remaining subject population of each pairwise interaction for each of the 1:m ratios. We identified interactions that were significantly stronger or weaker in the shift and stay conditions than at baseline by computing time-shifted surrogate data and deeming connections with a ratio of 2.42 (corresponding to $p < 0.01$) or higher as significant. Spurious connections were removed by estimating amplitude coupling between low and high frequencies and identifying triangle motifs (Siebenhühner et al., 2020). Shift and stay condition PAC were contrasted using a two-sided Wilcoxon signed-rank test with a statistical significance level $p < 0.05$ and corrected for multiple comparisons by removing the 5 % largest p-values. The trial order effect and behavioral correlations were again obtained with Spearman's r, as with oscillation amplitudes and phase synchrony.

Visualization and graph analysis

We visualized amplitude modulations across frequencies using amplitude TFRs, where the color scale represents the fraction of cortical parcels P with a statistically significant effect. Amplitude responses in TF

windows of interest were plotted onto inflated cortical surfaces. To investigate the spectral patterns of phase synchrony modulations associated with set-shifting, we also plotted the connection density K in TFRs.

Graph visualization was carried out for frequency-bands showing a significant effect in phase synchrony. For the selected frequency band in a condition contrast, we first constructed a group-level adjacency matrix that contained the average iPLV of significant edges across time and frequencies. To correct for false discoveries, we only included edges in the adjacency matrix that were significant in more than 15% of all TF bins in the window of interest. Each thresholded adjacency matrix defined a graph made up of nodes and edges, where nodes are cortical parcels and edges are the significant interactions between nodes. The graph metric degree was used to identify nodes that were central in the graphs and thus putatively played a key role in network communication.

While using iPLV to estimate inter-areal synchronization excludes the direct effects of zero-phase lagged signal mixing, spurious interactions still remain (Palva et al. 2018). We therefore removed edges between parcels for which the source reconstruction accuracy, fidelity, was below 0.1 (3.5 % of parcels). To further exclude spurious connections, we removed edges between parcels that exhibited the greatest signal leakage with their neighbors, measured with cross-patch PLV (fidelity radius greater than 0.4). A total of 17.8 % of all possible edges were thus excluded from the analyses. To further mitigate the contribution of spurious interactions caused by the concurrent presence of true interactions and linear mixing, a hyperedge-bundling approach was used (Wang et al. 2018) in the visualization of inter-areal network synchronization.

Graphs were then visualized on complete left and right flattened cerebral hemispheres that indicated simultaneous effects in oscillation amplitudes, revealing spectrally and temporally stable interactions that are likely to underlie the most important communication pathways. Lines indicated interareal interactions and were colored according to the connected parcels and networks. Spheres and annotations indicated parcels, with radii proportional to their degree, and borders proportional to their eigenvector centrality.

Results

Behavioral performance

In this study, 26 healthy participants completed a computer-based version of the Wisconsin Card Sorting Test (WCST) in which the active sorting rule (out of three possible rules) changed after every 5th trial. However, the subjects were not informed about this rule change interval, so that their task was to deduct the active rule solely from negative (shift) or positive feedback (stay). Participants made more early errors (N_{EE}; M = 119.3, SD = 27.8) during the first two trials of a new rule series than late errors (N_{LE}; M = 47.9, SD = 38.9; Fig. 2A), reflecting their rule learning. HRs increased with every trial within a rule set, showing a clear gradient in HRs from early to late trials (Fig. 2B). RTs were on average 102 ms longer in shift than stay trials ($T(25) = 6.01$, $p = 2.81e\text{-}6$) (Fig. 2C), meaning that participants reacted more slowly after having received negative feedback. Additionally, both RT_{shift} (r = 0.52, p = 0.0065) and RT_{stay} (r = 0.52, p = 0.0063), but not their difference RT_{shift} - RT_{stay} (r = 0.05, p = 0.7963), were positively correlated with N_{LE} across participants (Fig. 2D). Finally, we checked whether these results were confounded by age or sex. None of the outcome measures were significantly correlated with age: N_{LE} (r = 0.05, p = 0.827), RT_{shift} (r = 0.11, p = 0.573), RT_{stay} (r = 0.16, p = 0.422). There were also no differences between male and female participants in N_{LE} (T(24) = 1.220, p = 0.234), RT_{shift} (T(24) = 1.159, p = 0.258), or RT_{stay} (T(24) = 1.382, p = 0.180).

To investigate if these results were driven by higher responsiveness to positive or negative feedback, we implemented a sequential learning model with which we estimated the subject-wise parameters *r* (reward sensitivity), *p* (punishment sensitivity), *e* (exploration tendency), and *a* (anticipation tendency). We then used multiple linear regressions to reveal the explanatory value of these parameters on HRs, RTs and N_{LE}. The model was significant for HRs ($F(4,21) = 62.703$, $p < .001$, $R^2 = 0.923$) and N_{LE} ($F(4,21) = 70.818$, $p < .001$, $R^2 = 0.931$), but not RT_{stay} ($F(4,21) = 1.619$, $p = 0.207$, $R^2 = 0.236$) or RT_{shift} ($F(4,21) = 1.593$, $p = 0.213$, $R^2 = 0.233$). The regression equation for HR was thus $HR = 0.277 + (0.141r) + (0.315p) - (0.361e) + (0.430a)$ where all parameters but *r* were significant (*r*: p = 0.108, *e*: p = 0.017, *a*, *p*: p < 0.001). The number of late errors were explained by $N_{LE} = 153.2 - (62.5r) - (97.5p) + (191.8e) - (62.9a)$ with all parameters significant (*r*: p = 0.018, *p*, *e*, *a*: p < 0.001).

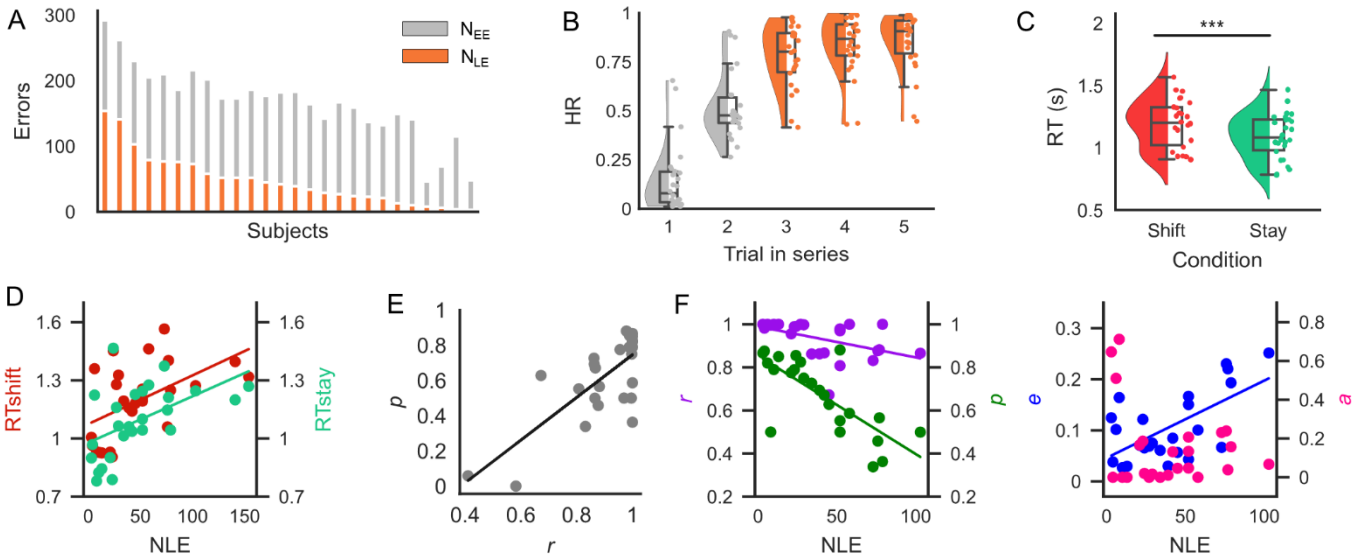

Figure 2. Behavioral results. A. Number of early and late errors by subjects. **B.** Averaged HRs for every trial in a rule set. The half violinplots and boxplots show the distribution and median values of HRs, and dots the subjects' means. **C.** The difference in RTs for shift and stay conditions between subjects. **D.** Scatterplot of the correlations of shift RTs and stay RTs with the number of late errors across participants. Colored fitting lines indicate the significant correlation of N_{LE} with RT_{shift} (red) and RT_{stay} (green). **E.** Correlation of the subject parameters r and p across participants when including the two outlier subjects. **F.** Correlations of all subject parameters with N_{LE} across participants after outlier exclusion.

Additionally, we correlated *r* and *p* across subjects (Fig. 2E, Pearson's r = 0.74, p < 0.001) which verified that responsivity to positive and negative feedback covaried within subjects. However, this was mainly driven by two outliers with low *r* and *p* values, so that their exclusion starkly reduced the correlation strength (Pearson's r = 0.41, p = 0.047). We therefore also plotted the correlation of each subject's parameters with N_{LE} after exclusion of the two outlier participants, showing that all parameters but *a* predicted N_{LE} (Fig. 2F; *r*: Pearson's r = -0.46, p = 0.023; *p*: Pearson's r = -0.75, p < 0.001; *e*: Pearson's r = 0.62, p = 0.001; *a*: Pearson's r = -0.28, p = 0.185).

Amplitude modulations in all frequency bands

Oscillation amplitudes were computed from individually source-reconstructed MEG data (Fig. 1C). To investigate if brain oscillation dynamics could underlie task switching behavior at the system level, we first compared shift and stay trials to the pre-stimulus baseline and then calculated significant differences between the two conditions (Fig. 3A, Wilcoxon signed-rank test, $p < 0.05$, $q = 0.08$). Shift and stay trials were both characterized by a strong sustained low-theta band (θ, 3–6 Hz) increase and a concurrent suppression of alpha (α, 7–13 Hz) and beta (β, 13–32 Hz) band amplitudes throughout the planning period. In addition, shift trials were also associated with an increase in gamma band (γ, 52–96 Hz) band amplitudes. These amplitude modulations were significantly stronger in shift than stay trials. Next, to study how amplitudes changed as participants learned the currently active rule, we correlated amplitudes with their trial order, i.e., the position of the trial within a rule set (Fig. 3B, Spearman's r, $p < 0.05$, $q = 0.08$). This revealed that participants showed smaller θ amplitudes between 0.9–1.8 s after feedback, and increased α–β amplitudes (0.5–1.35 s after feedback) as the rule set progressed, indicating that the θ–β amplitudes underwent a spectral transition from rule shifting towards staying at the correct rule. These effects had medium to strong effect sizes (Fig. 3C, θ: $p = 2.03e-34$, $r = 0.87$; α: $p = 6.88e-16$, $r = 0.57$; β: $p = 3.28e-26$, $r = 0.75$; γ: $p = 9.65e-31$, $r = 0.82$).

Differences in oscillation amplitude strengths in the θ band were widespread and found across parcels in frontal, temporal and visual cortices while in contrast the α and β amplitudes were suppressed over parietal areas with a concurrent amplitude increase in the left lateral (sub-)orbital sulcus and the bilateral primary visual areas , largely overlapping between the two frequency bands. Finally, γ increases were located in the left cingulate cortices, precuneus, insula and orbitofrontal cortex and the right calcarine sulcus and cuneus next to weak suppression in the postcentral sulci (Fig. 3D).

To chart the neural basis of variability in behavioral measures of cognitive flexibility, we investigated whether the condition-averaged amplitudes would predict differences across individuals in behavior and be explained by the parameters from our sequential learning model (Fig. 4). We first used the trial-to-trial rule certainty as a regressor for oscillation amplitudes, revealing that higher rule certainty was associated with smaller θ and larger α and β amplitudes (Fig. 4A), reflecting that the previously observed amplitude

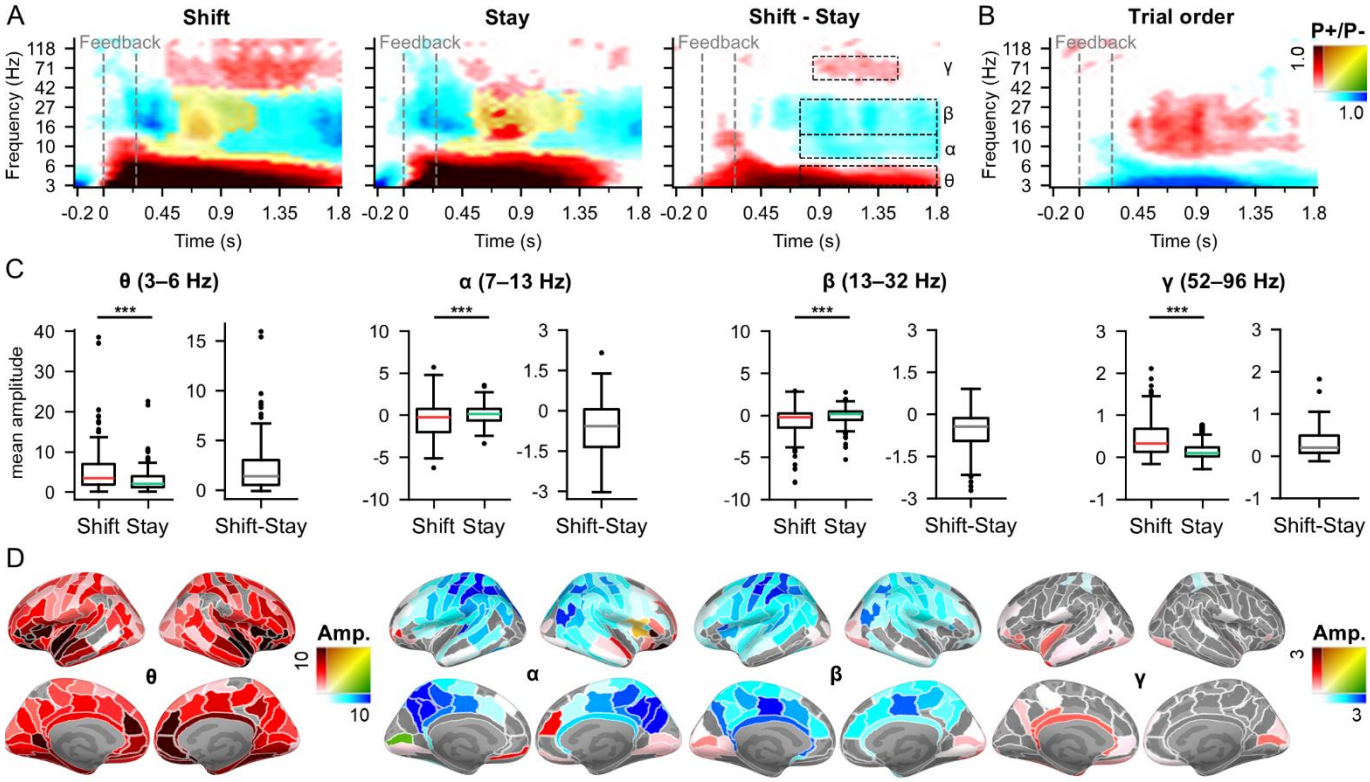

Figure 3. Oscillation amplitude effects. A. Group-averaged oscillations amplitudes of shift and stay trials compared to baseline, and their contrast. Color indicates the fraction of parcels (brain regions) (P) with a statistically significant effect (Wilcoxon signed-rank test, $p < 0.05$, FDR corrected, $q = 0.08$). The dashed black box indicates the time-frequency (TF) bins of interest during planning. **B.** The fraction of parcels whose amplitude significantly in- or decreases across a rule set (Spearman's r, $p < 0.05$, FDR corrected, $q = 0.08$). **C.** Boxplots indicating the mean differences between parcels in shift and stay trials in all TF windows of interest outlined in A. Asterisks indicate significant differences (Wilcoxon signed-rank test, $*p < 0.05$, $**p < 0.01$, $***p < 0.001$). The box of the boxplots indicates the range between the first quartile to the third quartile of the data, with a line at the median, while the whiskers extend to the farthest data point lying within 1.5x the inter-quartile range from the box, and fliers indicate all data points outside the whiskers' range. **D.** Mean amplitude differences between shift and stay trials as indicated by color gradients, plotted on an inflated brain surface of the Schaefer parcellation.

transition across a trial series was related to increased rule certainty. In comparison, the performance measures of individual variability in switching behavior, especially variability in N_{LE}, but also in RT_{shift} and RT_{stay}, were correlated positively only with α and β amplitudes while there was no effect in the θ amplitude unlike for rule certainty (Fig. 4B). These positive correlations with behavioral measures were found in the striate cortices, posterior parietal cortex (PPC), and in the medial PFC including insular and suborbital cortices (Fig. 4C). In addition, N_{LE}, and RT_{stay} were correlated negatively with γ amplitudes, meaning that subjects with larger γ-band activity made fewer late errors and gave faster responses, these correlations being widespread and arising from the parcels in the visual system, the intraparietal sulcus (IPS) of the PPC, and from both the lateral prefrontal cortex (PFC) and medial PFC including anterior cingulate cortices.

To then investigate whether these behavior-oscillation amplitude correlations could be explained by differences in feedback sensitivity, we correlated the amplitudes measures with subject-specific model parameters (Fig. 4D-E). Intriguingly, reward sensitivity *r* was predicted by transient biphasic modulation of α–β (11–29 Hz, 0.6 to 1.6 s after feedback onset) amplitudes, so that subjects that were more sensitive to positive feedback showed decreased right fronto-temporal β amplitudes and weaker α suppression in the bilateral cingulate cortices and left parietal cortex. The punishment sensitivity *p* and exploration tendency *e* were predicted similarly by stronger early α (7–11 Hz, 0.3 to 0.6 s) and β (13–27 Hz, 0.4 to 1 s) amplitudes, respectively, but in addition by sustained γ-band (43–143 Hz, 0.5 to 1.8 s) increases that were wide-spread, but the strongest over right IPS and bilateral cingulate cortices. In contrast, anticipation tendency *a* was predicted by distinct local oscillatory patterns, i.e., by early low-frequency (3–13 Hz, 0.4 to 0.9 s) and sustained θ (3–8 Hz, 1 to 1.8 s) amplitude increases. These effects were both strongest in the dorsomedial PFC, PPC, the right insula and visual parcels.

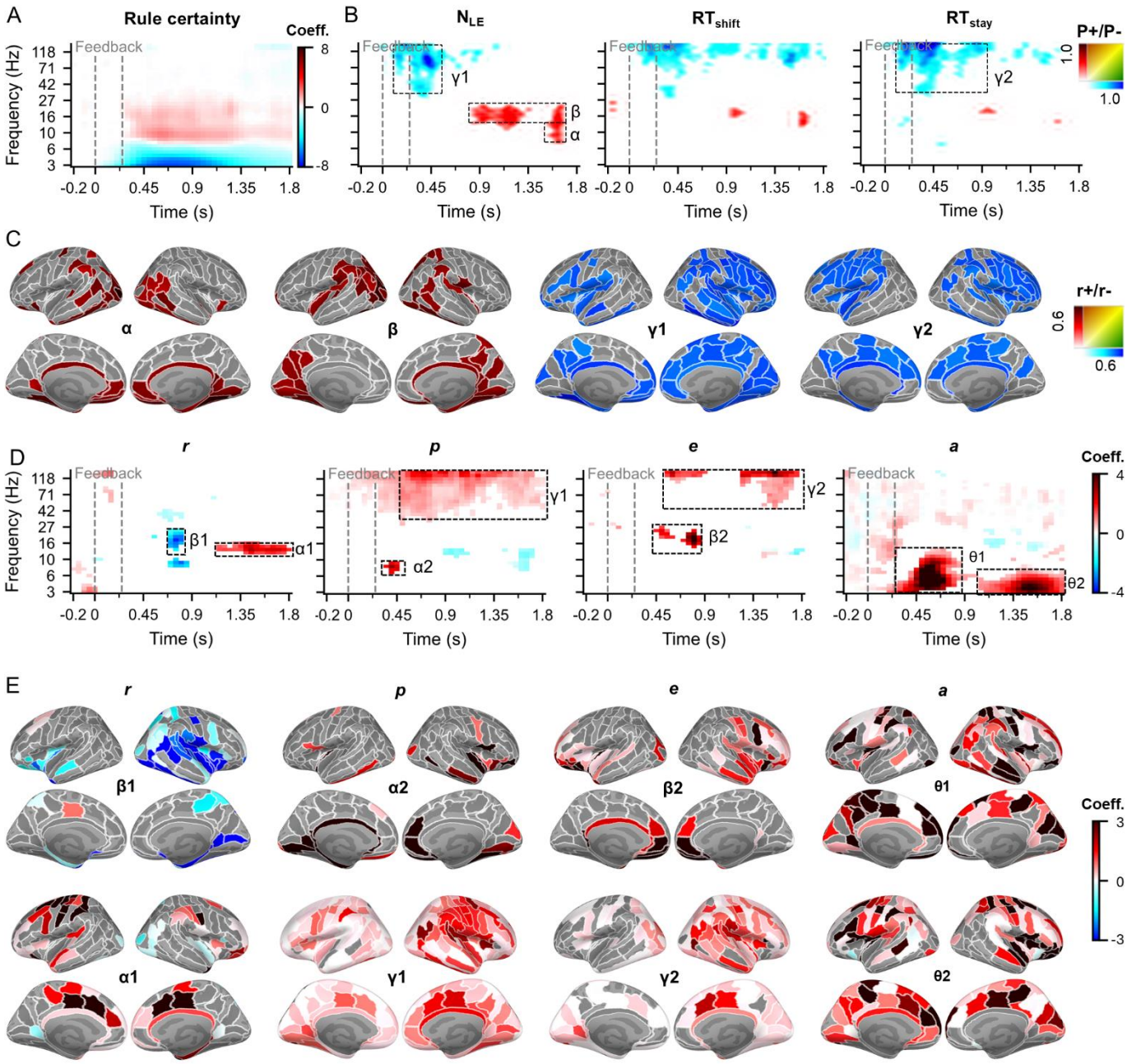

Figure 4. Amplitude in relation to performance and subject parameters. A. Oscillation amplitudes explained by increasing rule certainty within a trial series, where colors indicate the coefficients of parcels with a significant model fit (Linear Regression, $p < 0.05$, FDR corrected, $q = 0.08$). **B.** Correlation of parcel amplitudes with N_{LE}, and shift and stay RTs (Spearman's r, $p < 0.05$, FDR corrected, $q = 0.08$). **C.** Brain parcels with a significant correlation with N_{LE}. Color indicates the correlation coefficients. **D-E.** Model fit for each subject parameter with the mean amplitudes of shift and stay trials. The color expresses the coefficients of parcels with a significant model fit (Linear Regression, $p < 0.05$, FDR corrected, $q = 0.08$).

α desynchronization predicts N_{LE}

To resolve dynamics of oscillation-based functional connectivity in un-cued task-switching, we used a measure of inter-areal phase synchronization that indicates the statistical temporal regularities between brain areas. To this end, we computed inter-areal phase synchronization with iPLV between all cortical parcels and for all frequencies, separately for shift and stay trials against the baseline and then their difference between the two conditions (Fig. 5A, Wilcoxon signed-rank test, $p < 0.05$, $q = 0.0067$). Both the shift and stay conditions were characterized by strong θ (3–6 Hz) band synchronization that was sustained throughout the planning period, but also of α (9–15 Hz) desynchronization starting at 0.6 s after feedback. Both θ band synchronization and α desynchronization were stronger in shift than stay trials indicating that these synchronization dynamics relate to endogenous rule shifting. Next, we tested the relationship of phase synchronization with trial order by correlating the edge strength of every connection with the trial's position in the rule set, revealing a decrease in θ synchronization (Fig. 5B) and indicating that the synchronization decreased as the rule set progressed from shift towards stay trials with decreasing switching and planning demands. The comparison of edge strengths in the selected TF windows of interest (θ band, 0.6–1.35 s and α band, 0.35–0.7 s) showed that the largest differences between shift and stay conditions resulted in a medium effect size in the θ-band (Fig. 5C, Wilcoxon signed-rank test; $p = 0$, $r = 0.44$) and a small effect size in the α-band ($p = 3.34e\text{-}154$, $r = 0.18$). These effects were driven by functional connections within the visual function network and between visual and other networks (Fig. 5D).

To visualize the θ network architecture, we visualized the 200 strongest edges and nodes with the largest degrees (i.e., the number of edges with other nodes) in a graph (Fig. 5E). The graph consisted mostly of fronto-parietal edges, connecting the left lateral orbital sulcus (orbSla), midfrontal gyrus (mFG) and inferior frontal sulcus (iFS) with the temporal pole (Tpole), superior occipital gyrus (sOG) and cuneus (CN) of the primary visual areas in the left hemisphere as well as the lateral sulcus (laS), superior temporal sulcus (sTS), lateral occipitotemporal sulcus (laOTS), inferior occipital gyrus and sulcus (iO), and the superior occipital sulcus (sOS) and gyrus (sOG) in the right hemisphere.

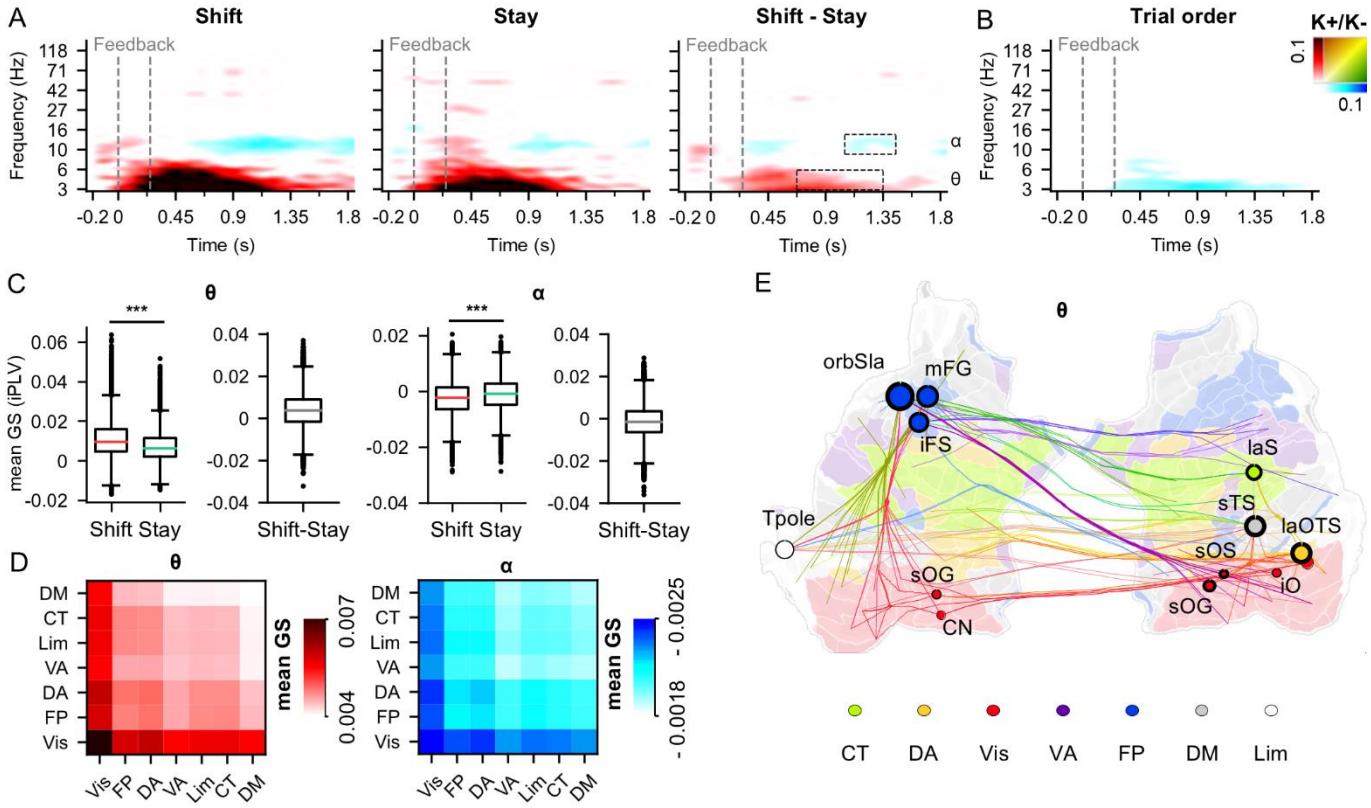

Figure 5. Phase synchrony (iPLV) results for shift and stay conditions. A. Interareal phase-synchronization during shift and stay trials compared to baseline and their contrast (Wilcoxon signed-rank test, $p < 0.05$, FDR corrected, $q = 0.0067$). Color indicates the connection density (K) of significant connections. **B.** Trial series effect showing the fraction of edges that significantly in- or decrease in phase synchronization across a rule set (Spearman's r, $p < 0.05$, FDR corrected, $q = 0.0067$). **C.** Boxplots showing the effect size of the difference between shift and stay trials, the asterisk indicating a highly significant difference. **D.** Mean graph strength (GS) of all edges according to their functional networks in the theta band (left) and alpha band (right). **E.** Theta-band (3–6 Hz, 0.7–1.3 s) matching graph showing the vertices with the highest source degree and the 150 edges with the strongest phase coupling.

As for the local oscillation amplitudes, we investigated whether mean strength of phase synchronization correlated across individuals with N_{LE}, RT_{shift} and RT_{stay} (Fig. 6A). We found that a smaller $N_{LE,}$ i.e., higher learning speed, was predicted by α (0.6–1.8 s) band desynchronization in a network comprised of edges between the suborbital sulcus (suborbS), superior and medial frontal gyri (sFG and mFG), inferior precentral

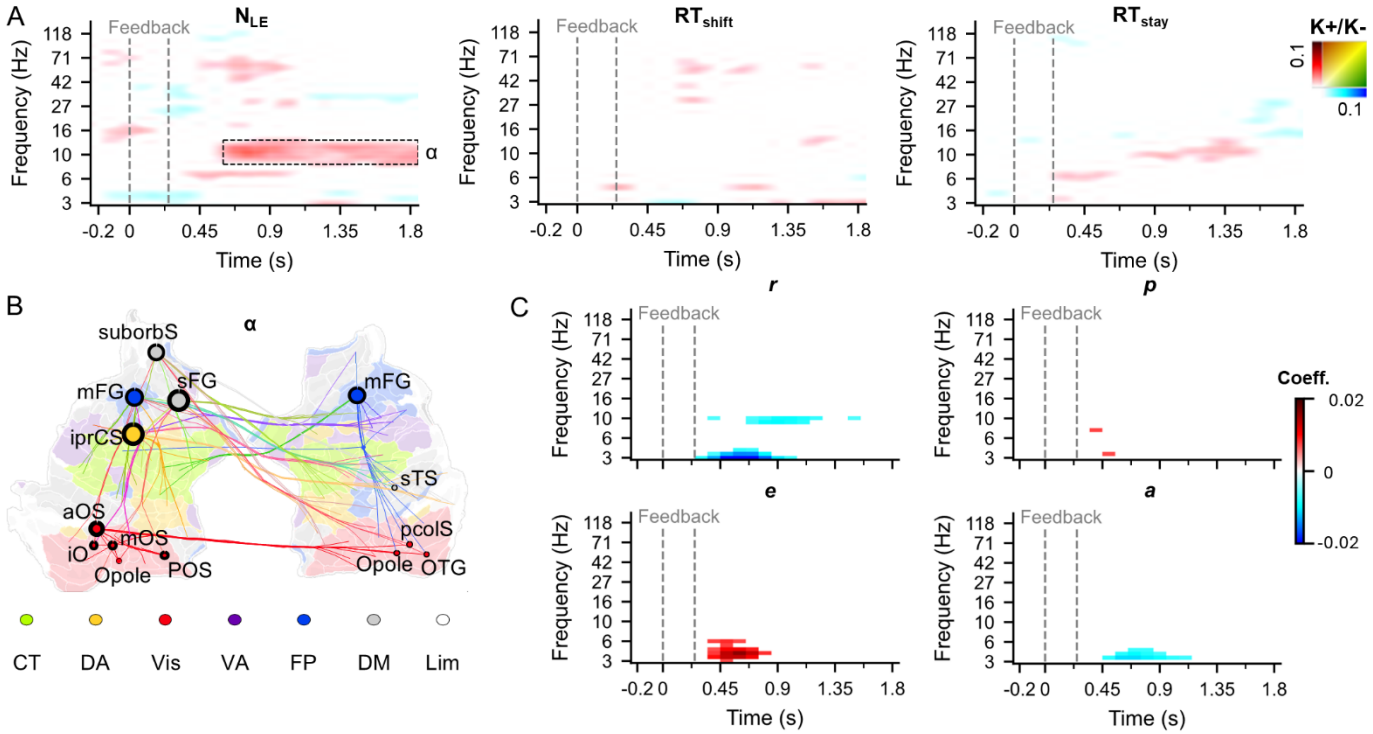

Figure 6. Phase synchrony (iPLV) correlations with performance and model fit of subject parameters. A. Correlation of phase synchronization with N_{LE}, and shift and stay RTs by frequency band (Spearman's r, $p < 0.05$, FDR corrected, $q = 0.0067$). **B.** Alpha-band (7–13 Hz, 0.6–1.8 s) matching graph showing the network of the nodes with the largest degrees and strongest edges correlating with the number of late errors. **C.** Model fit for each subject parameter with the mean edge strength of shift and stay trials. The color shade expresses the fraction of edges with a significant model fit (Linear Regression, $p < 0.05$, FDR corrected, $q = 0.0068$).

sulcus (iprCS), sTS, anterior occipital sulcus (aOS), mid-occipital sulci (mOS), iO, the bilateral occipital poles (Opole), parieto-occipital sulcus (POS), pcolS, and the occipitotemporal gyrus (OTG) (Fig. 6B).

Finally, we analyzed whether phase synchronization during the planning period would predict individual variability in reward sensitivity as assessed by differences in subject parameters (Fig. 6C). Increased reward sensitivity (*r*) and anticipation tendency (*a*) were predicted by smaller θ synchronization, whereas the opposite was true for a higher exploration tendency (*e*). Additionally, higher *r* values were also associated with stronger α desynchronization.

Phase-amplitude coupling of θ to α, β, and γ amplitudes predicts task-switching performance

In the previous analysis, we had established that local α to γ amplitudes and concurrent θ synchronization are relevant to endogenous task-switching. To study whether integration of these distinct processes could be achieved via cross-frequency interactions, we computed phase amplitude coupling (PAC) between low frequency concurrent θ oscillation phase and high frequency oscillation amplitudes (Fig. 7). We found that both shift and stay conditions were characterized by strong PAC between low to high-θ (3–8 Hz) phase and α–γ amplitudes (9–143 Hz, Fig. 7A). Additionally, θ-γ PAC was stronger in shift than stay trials and decreased over the course of a rule series (Fig. 7A–B). Post-hoc correlative analysis revealed that individuals with larger PAC of high-θ to all HFs predicted fewer N_{LE}, RT_{shift} and RT_{stay} (Fig. 7C). When plotting the strongest significant connections of the θ-γ PAC network (Fig. 7D), we found that the phase of the right medial frontal gyrus (mFG) and frontomarginal sulcus and gyrus (mrgF) were most coupled to γ amplitudes across the brain and especially to bilateral visual nodes. γ amplitudes of the left mFG and right superior parietal gyrus (sPG) were the most strongly coupled to the θ phase of frontal, parietal and visual nodes (Fig. 7D, right). These networks were consistent with the behaviorally relevant graphs (Supp. Fig. 1).

Discussion

Cognitive flexibility is the ability to quickly adapt behavior to changing environmental demands which is crucial for healthy cognitive functioning. Yet, individuals vary widely in their adaptation speed and accuracy, the precise physiological reasons for which remain elusive. Cognitive flexibility has previously been associated with prefrontal (Cohen & Cavanagh, 2011; Cooper et al., 2015; Cunillera et al., 2012; Sauseng et al., 2006; Sauseng & Liesefeld, 2020) and right centroparietal theta (θ, 3–8 Hz) band oscillations (Cooper et al., 2017) next to local modulations of alpha (α, 8–12 Hz) (Keitel et al., 2019; Kaiser et al., 2023), beta (β, 13–30 Hz) (Cunillera et al., 2012; Gladwin et al., 2006) and gamma (γ, 30–100 Hz) (Proskovec et al., 2019) band oscillation amplitudes over sensory and parietal areas. Yet, there is a limited understanding of the neural mechanisms of endogenous rule switching and its large inter-individual variability.

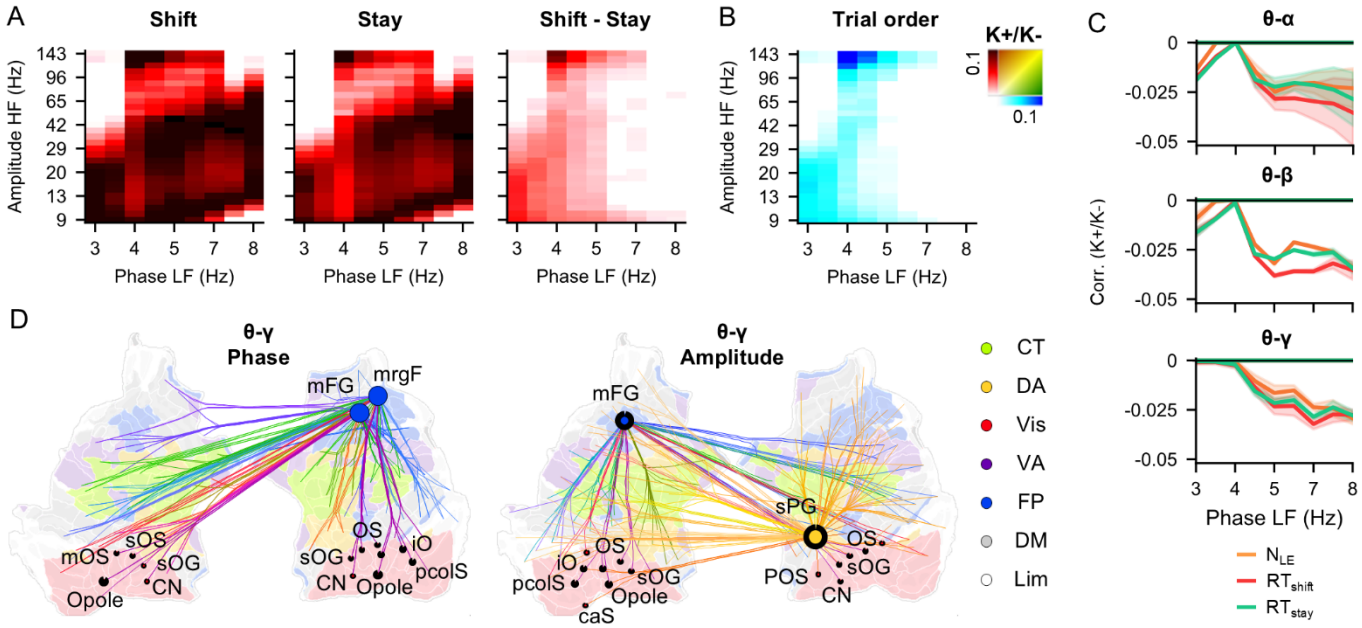

Figure 7. Phase amplitude coupling results for shift and stay conditions, trial order, and the correlations with performance. A. Phase amplitude coupling (PAC) between low-θ frequencies (LF) and high-α to γ frequencies (HF) during shift and stay trials compared to baseline (surrogate statistics, $p < 0.01$, corrected for spurious connections, $q = 0.035$) and their contrast (Wilcoxon signed-rank test, $p < 0.05$, FDR corrected, $q = 0.00389$). Color indicates the connection density (K) of significant connections. **B.** Trial series effect showing the fraction of edges with significant in- or decrease in PAC across a rule set (Spearman's r, $p < 0.05$, FDR corrected, $q = 0.00389$). **C.** Positive (K+) and negative (K-) tails of the correlations of PAC across frequency-band-averaged HFs with N_{LE}, RT_{shift} and RT_{stay} (Spearman's r, $p < 0.05$, $q = 0.00281$). **D.** Graphs showing the significant θ-γ PAC networks by largest degree of phase to amplitude coupling (left) and amplitude to phase coupling (right).

Here, using advanced analysis of MEG data and new computational modelling of behavioral performance, we demonstrate that both local oscillations and their large-scale networks predict individual variability in the task-switching accuracy as well as the sensitivity to feedback.

In line with previous research (Monsell, 2003), average RTs were shorter in stay than shift trials showing a delayed response associated with switching costs. Critically, we found large inter-subject variability in performance, revealing the heterogeneity of cognitive flexibility across individuals. This was especially visible in the number of errors made in the last 3 trials of a rule set (N_{LE}), reflecting the sizable differences

between subjects in the speed of adaptation to a rule change. In addition to these differences in learning speed, we established that there was a large interindividual variability in switching speed as measured by RTs of trials following negative feedback (RT_{shift}) and positive feedback (RT_{stay}). These three behavioral measures were positively correlated within subjects, thus revealing that there was no speed-accuracy trade-off in line with previous task-switching literature (e.g., Kiesel et al., 2010; Vandierendonck et al., 2010; Vandierendonck, 2017). The correlation of N_{LE}, RT_{shift} and RT_{stay}, further demonstrated that these behaviors are likely due to a shared neural mechanism.

Using a new computational model based on the model by Bishara and colleagues (2010) to model individual differences in sequential learning, we found that reward sensitivity, punishment sensitivity, and exploration tendency were highly predictive of subjects' HR and N_{LE}, and were thus well-suited to explore the distinct neuronal mechanisms of positive and negative feedback sensitivity leading to the large variability in un-cued task-switching. Importantly, this variability was not driven by demographic factors such as sex or age in our sample likely due to the young age of our participants (Boone et al., 1993; Rhodes, 2004). All interindividual differences in oscillatory modulations can therefore be expected to reflect actual differences in cognitive flexibility.

In this study, we analyzed the frequency-dependent neuronal circuitry underlying cognitive flexibility in un-cued task-switching during the WCST. To this end, we mapped changes in local oscillation amplitudes during the planning period following feedback and found that the amplitudes differed in all frequency bands between the shift and stay conditions. While our results generally align with previous findings for changes in the different frequency bands in externally cued task-switching, we show here for the first time the distinction of amplitude modulations associated with internally guided rule learning over time and how the variability in oscillation dynamics explain the inter-individual variability in performance measures. In particular, we found amplitude increases compared to baseline in the θ (3–6 Hz) and γ (52–96 Hz) band oscillations, alongside α (8–13 Hz) and β (13–32 Hz) band suppression over the PPC. All of these amplitude modulations were enhanced in shift conditions compared to stay trials.

Interestingly, fewer N_{LE} and faster processing speed were correlated with posterior α and β suppression as well as increased fronto-temporal γ, but not θ amplitudes across individuals. Similarly, subjects with a better

ability to tune their responses using either positive or negative feedback differed in their α, β, and γ amplitudes. One central mechanism associated with shift trials as well as enhanced performance was therefore a sustained increase in γ amplitudes over frontal and parietal parcels. This was driven by higher levels of punishment sensitivity and exploration tendency, indicating that subjects responding more strongly to negative feedback displayed larger γ amplitudes, leading to fewer late errors and shorter RTs. So far, there has been only sparse evidence linking γ amplitudes to cognitive control performance in humans, where increased γ amplitudes have been associated with enhanced behavioral switching (Proskovec et al., 2019) and faster reorienting of attention (Spooner et al., 2020), as opposed to diminished γ amplitudes and impaired cognitive control abilities in schizophrenia (Cho et al., 2006; Minzenberg et al., 2010). While it is generally assumed that γ amplitudes reflect processing of sensory information in cognitive tasks (Fitzgibbon et al., 2004; Honkanen et al., 2015; Jensen et al., 2007), we provide novel evidence for their role in un-cued task switching and show that their variance across subjects is directly linked to performance differences in the WCST.

On the other hand, we found stronger prefrontal θ amplitudes in the shift than in the stay condition, which have previously been connected to exertion of cognitive control (G. Gratton et al., 2018), conflict monitoring (Sauseng & Liesefeld, 2020; Cohen & Cavanagh, 2011) and anticipatory task switching (Cooper et al., 2015; Cunillera et al., 2012; Sauseng et al., 2006; Cooper et al., 2017). However, we found that increased θ amplitudes were not associated with performance differences in this study and thus seemed to have an indirect role in task switching. Indeed, θ amplitudes predicted rule learning and increased rule certainty across a trial series, on top of larger θ amplitudes being explained by a tendency to anticipate rule changes. Our results thus indicate that increased θ amplitudes are not a facilitating mechanism for behavioral switching per se, but rather characterize the subject's understanding of the task, so that upcoming rule changes can be better anticipated and new rules learnt quickly.

In addition to γ, we also found the amplitude modulations in the other frequency bands to be crucially involved in un-cued task switching. In contrast to facilitated θ and γ band oscillations, α and β band suppression over the PPC were stronger in shift than stay trials. This decrease in their mean amplitudes was predictive of N_{LE} and RTs across individuals in line with the role of posterior α suppression in previous

cued task-switching studies (Capizzi et al., 2020; Foxe et al., 2014; Murphy et al., 2016; Verstraeten & Cluydts, 2002). We also found that these amplitude modulations were crucially driven by the positive feedback sensitivity *r*, so that individuals with a higher tendency to stay at the current rule exhibited a stronger β suppression but higher α amplitudes. We therefore postulate that decreased α amplitudes might be due to increased allocation of attention (Thut et al. 2006; Jensen and Mazaheri 2010; Haegens et al. 2011) to the sensory domain relevant to the switch-task (Cooper et al., 2016; Proskovec et al., 2019; Rapela et al., 2012; Sauseng et al., 2006; Wu et al., 2015) and putatively modulating neuronal excitability in visual and sensorimotor tasks (Balestrieri and Busch 2022; Haegens et al. 2011; Lange et al. 2013; Iemi et al. 2017). β suppression on the other hand has been shown in connection with switch cues, particularly over posterior-occipital regions and the left premotor cortex, which has been interpreted within a motor control framework (Cunillera et al., 2012; Cooper et al., 2017, 2019; Gladwin et al., 2006). Additionally, suppression in β amplitudes has been connected to inhibitory control in task switching (Cunillera et al., 2012; Gladwin et al., 2006) and in VWM (Wessel and Anderson, 2024; Lundqvist et al., 2024). Therefore, α and β band suppression might improve cognitive flexibility in different manners (Capizzi et al., 2020; Cooper et al., 2016; Gratton et al., 2018).

In this study, we carried out a whole-brain analysis of phase synchronization networks during the WCST. Both shift and stay trials showed a pattern of sustained θ phase synchronization and α desynchronization, which were stronger in the shift condition. However, stronger prefrontal θ-band network synchronization was not directly linked to performance differences. Indeed, θ-band synchronization was increased in subjects with lower levels of reward sensitivity and anticipation tendency, but greater exploration tendency. Our results therefore provide new evidence that large-scale networks of prefrontal θ band network synchronization might be a crucial neural inter-areal mechanism for rule exploration and internally guided flexible task-switching, but not for feedback-driven rule learning.

On the other hand, we also found prefrontal α desynchronization to be stronger in task switching, which correlated with N_{LE} across subjects so that individuals with more α desynchronization made fewer errors, and were also more sensitive to positive feedback. This is surprising as larger α synchronization is associated with higher top-down attention in attention tasks (Doesburg et al., 2009; Lobier et al., 2018;

Mima et al., 2001) and VWM (Palva et al., 2010, Sauseng et al., 2005, von Stein et al., 2000, Zanto et al., 2011) and is typically positively correlated with better task performance (Ericson et al., 2024; Sattelberger et al., 2024). One possible explanation for our result is that disengagement of the α network served as a reset of the internal top-down goal (i.e., the current sorting rule). This is supported by some earlier studies in which α desynchronization during visual tasks was related to the tuning of attention in presence of competing sensory stimuli (Gross et al., 2004; Mylonas et al., 2016; Rodriguez et al., 1999). In our study, the α desynchronization may therefore reflect disengagement from the previously chosen wrong rule.

Finally, we also investigated the cross-frequency interactions of the local amplitude modulations and phase synchronization that we found in un-cued task switching. We found θ phase coupling to all amplitudes to play a crucial role in task-switching accuracy and speed. Particularly, the θ phase of the right dorsolateral PFC was significantly coupled to left PFC and bilateral parietal and visual γ amplitudes. Furthermore, we found stronger θ-γ PAC to predict fewer N_{LE}, and shorter RT_{shift} and RT_{stay}, along with PAC in the other frequency bands. While there is emerging evidence pointing out the significance of nested oscillations and specifically θ-γ coupling for cognitive functioning in attention and working memory (Abubaker et al., 2021; Berger et al., 2019; Brooks et al., 2020; de Lara et al., 2018; Hermiller et al., 2020; Lisman & Jensen, 2013; Spooner et al., 2020) and global cognitive control (Alekseichuk et al., 2016; Bramson et al., 2020; Moser et al., 2024; Riddle et al., 2021; Turi et al., 2020), we prove here for the first time its role in un-cued task switching. It has been proposed that θ-γ PAC could allow for rapid communication between brain areas to implement pro- and reactive cognitive control (Pagnotta et al., 2024; Verguts, 2017; Voytek et al., 2015). Consequently, θ-γ coupling appears to coordinate the top-down selection of the correct rule set in the WCST. This interpretation is further supported by our finding that θ-γ PAC decreased over the course of a rule series. Our study therefore extends previous notions of the role of prefrontal θ amplitudes as a cognitive control mechanism and provides detailed insights into the significance of θ phase synchronization and its dynamic interactions across anatomy and frequencies.

Conclusions

Taken together, our results show that the great inter-individual variability in cognitive flexibility in the WCST depends on multiple concurrent modulations of oscillation amplitudes and their phase interactions, which are predicted by differences in individual feedback sensitivity. Higher learning speed as measured with NLE was predicted by local γ band amplitude increases and parietal α and β band suppression, which were distinctly explained by higher sensitivity to negative and positive feedback, respectively. We further revealed the crucial role of sustained frontoparietal α network desynchronization for learning speed, which was strongly associated with increased reward sensitivity, as well as the role of theta-gamma phase amplitude coupling for inter-areal communication in cognitive flexibility. Our results therefore provide novel insights that differences in the individual sensitivity to positive and negative feedback explain not only faster and more accurate rule learning in the WCST but are also predictive of distinct local and large-scale oscillatory network mechanisms.

References

Abubaker, M., Al Qasem, W., & Kvašňák, E. (2021). Working Memory and Cross-Frequency Coupling of Neuronal Oscillations [Review]. *Frontiers in Psychology*, *12*. https://doi.org/10.3389/fpsyg.2021.756661

Alekseichuk, I., Turi, Z., Amador de Lara, G., Antal, A., & Paulus, W. (2016). Spatial Working Memory in Humans Depends on Theta and High Gamma Synchronization in the Prefrontal Cortex. *Current Biology*, *26*(12), 1513-1521. https://doi.org/https://doi.org/10.1016/j.cub.2016.04.035

Baillet, S. (2017). Magnetoencephalography for brain electrophysiology and imaging. *Nature Neuroscience*, *20*(3), 327-339.

Barcelo, F. (2003). The Madrid card sorting test (MCST): a task switching paradigm to study executive attention with event-related potentials. *Brain Research Protocols*, *11*(1), 27-37.

Berg, E. A. (1948). A Simple Objective Technique for Measuring Flexibility in Thinking. *The Journal of General Psychology*, *39*(1), 15-22. https://doi.org/10.1080/00221309.1948.9918159

Berger, B., Griesmayr, B., Minarik, T., Biel, A. L., Pinal, D., Sterr, A., & Sauseng, P. (2019). Dynamic regulation of interregional cortical communication by slow brain oscillations during working memory. *Nature Communications*, *10*(1), 4242.

Biel, A. L., Minarik, T., & Sauseng, P. (2021). EEG cross-frequency phase synchronization as an index of memory matching in visual search. *NeuroImage*, *235*, 117971.

Bissonette, G. B., Powell, E. M., & Roesch, M. R. (2013). Neural structures underlying set-shifting: Roles of medial prefrontal cortex and anterior cingulate cortex. *Behavioural Brain Research*, *250*, 91-101. https://doi.org/10.1016/j.bbr.2013.04.037

Boone, K. B., Ghaffarian, S., Lesser, I. M., Hill-Gutierrez, E., & G. Berman, N. (1993). Wisconsin card sorting test performance in healthy, older adults: Relationship to age, sex, education, and IQ. *Journal of Clinical Psychology*, *49*(1), 54-60. https://doi.org/https://doi.org/10.1002/1097-4679(199301)49:1<54::AID-JCLP2270490108>3.0.CO;2-6

Bramson, B., den Ouden, H. E., Toni, I., & Roelofs, K. (2020). Improving emotional-action control by targeting long-range phase-amplitude neuronal coupling. *eLife*, *9*, e59600.

Brass, M., Ullsperger, M., Knoesche, T. R., Cramon, D. Y. v., & Phillips, N. A. (2005). Who Comes First? The Role of the Prefrontal and Parietal Cortex in Cognitive Control. *Journal of Cognitive Neuroscience*, *17*(9), 1367-1375. https://doi.org/10.1162/0898929054985400

Brooks, H., Goodman, M. S., Bowie, C. R., Zomorrodi, R., Blumberger, D. M., Butters, M. A., Daskalakis, Z. J., Fischer, C. E., Flint, A., Herrmann, N., Kumar, S., Mah, L., Mulsant, B. H., Pollock, B. G., Voineskos, A. N., Rajji, T. K., Mulsant, B. H., Rajji, T. K., Herrmann, N., . . . on behalf of the, P.-M. D. S. G. (2020). Theta–gamma coupling and ordering information: a stable brain–behavior relationship across cognitive tasks and clinical conditions. *Neuropsychopharmacology*, *45*(12), 2038-2047. https://doi.org/10.1038/s41386-020-0759-z

Buckley, M. J., Mansouri, F. A., Hoda, H., Mahboubi, M., Browning, P. G., Kwok, S. C., Phillips, A., & Tanaka, K. (2009). Dissociable components of rule-guided behavior depend on distinct medial and prefrontal regions. *Science*, *325*(5936), 52-58.

Capizzi, M., Ambrosini, E., Arbula, S., & Vallesi, A. (2020). Brain oscillatory activity associated with switch and mixing costs during reactive control. *Psychophysiology*, *57*(11), e13642. https://doi.org/https://doi.org/10.1111/psyp.13642

Cavanagh, J. F., Cohen, M. X., & Allen, J. J. B. (2009). Prelude to and Resolution of an Error: EEG Phase Synchrony Reveals Cognitive Control Dynamics during Action Monitoring. *The Journal of Neuroscience*, *29*(1), 98. https://doi.org/10.1523/JNEUROSCI.4137-08.2009

Cavanagh, J. F., & Frank, M. J. (2014). Frontal theta as a mechanism for cognitive control. *Trends in Cognitive Sciences*, *18*(8), 414-421. https://doi.org/https://doi.org/10.1016/j.tics.2014.04.012

Cho, R., Konecky, R., & Carter, C. S. (2006). Impairments in frontal cortical γ synchrony and cognitive control in schizophrenia. *Proceedings of the National Academy of Sciences*, *103*(52), 19878-19883.

Cohen, M. X. (2011). Error-related medial frontal theta activity predicts cingulate-related structural connectivity. *NeuroImage*, *55*(3), 1373-1383. https://doi.org/https://doi.org/10.1016/j.neuroimage.2010.12.072

Cohen, M. X., & Cavanagh, J. F. (2011). Single-Trial Regression Elucidates the Role of Prefrontal Theta Oscillations in Response Conflict [Original Research]. *Frontiers in Psychology*, *2*. https://doi.org/10.3389/fpsyg.2011.00030

Cohen, M. X., Elger, C. E., & Ranganath, C. (2007). Reward expectation modulates feedback-related negativity and EEG spectra. *NeuroImage*, *35*(2), 968-978.

Cooper, P. S., Wong, A. S. W., Fulham, W. R., Thienel, R., Mansfield, E., Michie, P. T., & Karayanidis, F. (2015). Theta frontoparietal connectivity associated with proactive and reactive cognitive control processes. *NeuroImage*, *108*, 354-363. https://doi.org/10.1016/j.neuroimage.2014.12.028

Cooper, P. S., Wong, A. S. W., McKewen, M., Michie, P. T., & Karayanidis, F. (2017). Frontoparietal theta oscillations during proactive control are associated with goal-updating and reduced behavioral variability. *Biological Psychology*, *129*, 253-264. https://doi.org/10.1016/j.biopsycho.2017.09.008

Cunillera, T., Fuentemilla, L., Periañez, J., Marco-Pallarès, J., Krämer, U. M., Càmara, E., Münte, T. F., & Rodríguez-Fornells, A. (2012). Brain oscillatory activity associated with task switching and feedback processing. *Cognitive, Affective, & Behavioral Neuroscience*, *12*(1), 16-33. https://doi.org/10.3758/s13415-011-0075-5

D'Andrea, A., Chella, F., Marshall, T. R., Pizzella, V., Romani, G. L., Jensen, O., & Marzetti, L. (2019). Alpha and alpha-beta phase synchronization mediate the recruitment of the visuospatial attention network through the Superior Longitudinal Fasciculus. *NeuroImage*, *188*, 722-732. https://doi.org/10.1016/j.neuroimage.2018.12.056

de Lara, G. A., Alekseichuk, I., Turi, Z., Lehr, A., Antal, A., & Paulus, W. (2018). Perturbation of theta-gamma coupling at the temporal lobe hinders verbal declarative memory. *Brain Stimulation*, *11*(3), 509-517.

Doesburg, S. M., Green, J. J., McDonald, J. J., & Ward, L. M. (2009). From local inhibition to long-range integration: A functional dissociation of alpha-band synchronization across cortical scales in visuospatial attention. *Brain Research*, *1303*, 97-110. https://doi.org/https://doi.org/10.1016/j.brainres.2009.09.069

Dosenbach, N. U., Fair, D. A., Cohen, A. L., Schlaggar, B. L., & Petersen, S. E. (2008). A dual-networks architecture of top-down control. *Trends Cogn Sci*, *12*(3), 99-105. https://doi.org/10.1016/j.tics.2008.01.001

Dosenbach, N. U. F., Fair, D. A., Miezin, F. M., Cohen, A. L., Wenger, K. K., Dosenbach, R. A. T., Fox, M. D., Snyder, A. Z., Vincent, J. L., Raichle, M. E., Schlaggar, B. L., & Petersen, S. E. (2007). Distinct brain networks for adaptive and stable task control in humans. *Proceedings of the National Academy of Sciences*, *104*(26), 11073-11078. https://doi.org/doi:10.1073/pnas.0704320104

Ericson, J., Palva, S., Palva, M., & Klingberg, T. (2024). Strengthening of alpha synchronization is a neural correlate of cognitive transfer. *Cerebral Cortex*, *34*(2). https://doi.org/10.1093/cercor/bhad527

Foxe, J. J., Murphy, J. W., & De Sanctis, P. (2014). Throwing out the rules: anticipatory alpha-band oscillatory attention mechanisms during task-set reconfigurations. *European Journal of Neuroscience*, *39*(11), 1960-1972. https://doi.org/https://doi.org/10.1111/ejn.12577

Fries, P. (2015). Rhythms for Cognition: Communication through Coherence [Review]. *Neuron*, *88*(1), 220-235. https://doi.org/10.1016/j.neuron.2015.09.034

Gladwin, T. E., Lindsen, J. P., & de Jong, R. (2006). Pre-stimulus EEG effects related to response speed, task switching and upcoming response hand. *Biological Psychology*, *72*(1), 15-34. https://doi.org/https://doi.org/10.1016/j.biopsycho.2005.05.005

Gratton, C., Sun, H., & Petersen, S. E. (2018). Control networks and hubs. *Psychophysiology*, *55*(3), e13032. https://doi.org/https://doi.org/10.1111/psyp.13032

Gratton, G., Cooper, P., Fabiani, M., Carter, C. S., & Karayanidis, F. (2018). Dynamics of cognitive control: Theoretical bases, paradigms, and a view for the future. *Psychophysiology*, *55*(3), e13016. https://doi.org/https://doi.org/10.1111/psyp.13016

Guarino, A., Forte, G., Giovannoli, J., & Casagrande, M. (2020). Executive functions in the elderly with mild cognitive impairment: a systematic review on motor and cognitive inhibition, conflict control and cognitive flexibility. *Aging & Mental Health*, *24*(7), 1028-1045. https://doi.org/10.1080/13607863.2019.1584785

Haegens, S., Händel, B. F., & Jensen, O. (2011). Top-Down Controlled Alpha Band Activity in Somatosensory Areas Determines Behavioral Performance in a Discrimination Task. The Journal of Neuroscience, 31(14), 5197-5204. https://doi.org/10.1523/jneurosci.5199-10.2011

Hari, R., & Salmelin, R. (1997). Human cortical oscillations: a neuromagnetic view through the skull. *Trends in Neurosciences*, *20*(1), 44-49.

Hermiller, M. S., Chen, Y. F., Parrish, T. B., & Voss, J. L. (2020). Evidence for immediate enhancement of hippocampal memory encoding by network-targeted theta-burst stimulation during concurrent fMRI. *Journal of Neuroscience*, *40*(37), 7155-7168.

Huang, A. S., Wimmer, R. D., Lam, N. H., Wang, B. A., Suresh, S., Roeske, M. J., Pleger, B., Halassa, M. M., & Woodward, N. D. (2024). A prefrontal thalamocortical readout for conflict-related executive dysfunction in schizophrenia. *Cell Reports Medicine*, *5*(11). https://doi.org/10.1016/j.xcrm.2024.101802

Jensen, O., Kaiser, J., & Lachaux, J.-P. (2007). Human gamma-frequency oscillations associated with attention and memory. *Trends in Neurosciences*, *30*(7), 317-324. https://doi.org/https://doi.org/10.1016/j.tins.2007.05.001

Kaiser, J., Oberschulte, J. M., Heckmann, M., & Schütz-Bosbach, S. (2023). Flexible Changes in Attentional Focus and Task Rules Rely on A Shared Set of Frontoparietal Oscillatory Dynamics. *Journal of Cognitive Neuroscience*, *35*(7), 1075-1091. https://doi.org/10.1162/jocn_a_02002

Keitel, C., Keitel, A., Benwell, C. S. Y., Daube, C., Thut, G., & Gross, J. (2019). Stimulus-Driven Brain Rhythms within the Alpha Band: The Attentional-Modulation Conundrum. *The Journal of Neuroscience*, *39*(16), 3119-3129. https://doi.org/10.1523/jneurosci.1633-18.2019

Kiesel, A., Steinhauser, M., Wendt, M., Falkenstein, M., Jost, K., Philipp, A. M., & Koch, I. (2010). Control and interference in task switching—A review. *Psychological Bulletin*, *136*(5), 849-874. https://doi.org/10.1037/a0019842

Kupis, L., Goodman, Z. T., Kornfeld, S., Hoang, S., Romero, C., Dirks, B., Dehoney, J., Chang, C., Spreng, R. N., Nomi, J. S., & Uddin, L. Q. (2021). Brain Dynamics Underlying Cognitive Flexibility Across the Lifespan. *Cerebral Cortex*, *31*(11), 5263-5274. https://doi.org/10.1093/cercor/bhab156

Lisman, John E., & Jensen, O. (2013). The Theta-Gamma Neural Code. *Neuron*, *77*(6), 1002-1016. https://doi.org/10.1016/j.neuron.2013.03.007

Lobier, M., Palva, J. M., & Palva, S. (2018). High-alpha band synchronization across frontal, parietal and visual cortex mediates behavioral and neuronal effects of visuospatial attention. *NeuroImage*, *165*, 222-237. https://doi.org/https://doi.org/10.1016/j.neuroimage.2017.10.044

Mansfield, E. L., Karayanidis, F., & Cohen, M. X. (2012). Switch-Related and General Preparation Processes in Task-Switching: Evidence from Multivariate Pattern Classification of EEG Data. *The Journal of Neuroscience*, *32*(50), 18253-18258. https://doi.org/10.1523/jneurosci.0737-12.2012

Martin, J. E. (2006). *Card sorting test performance: the role of visual working memory and the effect of visual feedback* University Of Tasmania].

Miles, S., Howlett, C. A., Berryman, C., Nedeljkovic, M., Moseley, G. L., & Phillipou, A. (2021). Considerations for using the Wisconsin Card Sorting Test to assess cognitive flexibility. *Behavior Research Methods*, *53*(5), 2083-2091. https://doi.org/10.3758/s13428-021-01551-3

Mima, T., Oluwatimilehin, T., Hiraoka, T., & Hallett, M. (2001). Transient Interhemispheric Neuronal Synchrony Correlates with Object Recognition. *The Journal of Neuroscience*, *21*(11), 3942-3948. https://doi.org/10.1523/jneurosci.21-11-03942.2001

Minzenberg, M. J., Firl, A. J., Yoon, J. H., Gomes, G. C., Reinking, C., & Carter, C. S. (2010). Gamma oscillatory power is impaired during cognitive control independent of medication status in first-episode schizophrenia. *Neuropsychopharmacology*, *35*(13), 2590-2599.

Monsell, S. (2003). Task switching. *Trends in Cognitive Sciences*, *7*(3), 134-140.

Moser, J. S., Munia, T. T. K., Louis, C. C., Anderson, G. E., & Aviyente, S. (2024). Errors elicit frontoparietal theta-gamma coupling that is modulated by endogenous estradiol levels. *International Journal of Psychophysiology*, *197*, 112299. https://doi.org/https://doi.org/10.1016/j.ijpsycho.2024.112299

Murphy, J. W., Foxe, J. J., & Molholm, S. (2016). Neuro-oscillatory mechanisms of intersensory selective attention and task switching in school-aged children, adolescents and young adults. *Developmental Science*, *19*(3), 469-487. https://doi.org/https://doi.org/10.1111/desc.12316

Pagnotta, M. F., Riddle, J., & D'Esposito, M. (2024). Multimodal neuroimaging of hierarchical cognitive control. *Biological Psychology*, *193*, 108896. https://doi.org/https://doi.org/10.1016/j.biopsycho.2024.108896

Palva, J. M., Wang, S. H., Palva, S., Zhigalov, A., Monto, S., Brookes, M. J., Schoffelen, J. M., & Jerbi, K. (2018). Ghost interactions in MEG/EEG source space: A note of caution on inter-areal coupling measures. *NeuroImage*, *173*, 632-643. https://doi.org/10.1016/j.neuroimage.2018.02.032

Palva, S., & Palva, J. M. (2012). Discovering oscillatory interaction networks with M/EEG: challenges and breakthroughs. *Trends Cogn Sci*, *16*(4), 219-230. https://doi.org/10.1016/j.tics.2012.02.004

Panikratova, Y. R., Vlasova, R. M., Akhutina, T. V., Korneev, A. A., Sinitsyn, V. E., & Pechenkova, E. V. (2020). Functional connectivity of the dorsolateral prefrontal cortex contributes to different components of executive functions. *International Journal of Psychophysiology*, *151*, 70-79. https://doi.org/https://doi.org/10.1016/j.ijpsycho.2020.02.013

Peltz, C. B., Gratton, G., & Fabiani, M. (2011). Age-Related Changes in Electrophysiological and Neuropsychological Indices of Working Memory, Attention Control, and Cognitive Flexibility [Original Research]. *Frontiers in Psychology*, *2*. https://doi.org/10.3389/fpsyg.2011.00190

Peylo, C., Friedrich, E. V., Minarik, T., Biel, A. L., & Sauseng, P. (2022). Theta: gamma phase coupling and evoked gamma activity reflect the fidelity of mental templates during memory matching in visual perception. *Cerebral Cortex*, *32*(19), 4156-4171.

Proskovec, A. L., Wiesman, A. I., & Wilson, T. W. (2019). The strength of alpha and gamma oscillations predicts behavioral switch costs. *NeuroImage*, *188*, 274-281. https://doi.org/https://doi.org/10.1016/j.neuroimage.2018.12.016

Ravizza, S. M., & Ciranni, M. A. (2002). Contributions of the Prefrontal Cortex and Basal Ganglia to Set Shifting. *Journal of Cognitive Neuroscience*, *14*(3), 472-483. https://doi.org/10.1162/089892902317361985

Rhodes, M. G. (2004). Age-related differences in performance on the Wisconsin card sorting test: a meta-analytic review. *Psychology and aging*, *19*(3), 482.

Riddle, J., McFerren, A., & Frohlich, F. (2021). Causal role of cross-frequency coupling in distinct components of cognitive control. *Progress in Neurobiology*, *202*, 102033. https://doi.org/https://doi.org/10.1016/j.pneurobio.2021.102033

Riddle, J., Scimeca, J. M., Cellier, D., Dhanani, S., & D'Esposito, M. (2020). Causal Evidence for a Role of Theta and Alpha Oscillations in the Control of Working Memory. *Current Biology*, *30*(9), 1748-1754.e1744. https://doi.org/https://doi.org/10.1016/j.cub.2020.02.065

Rikhye, R. V., Gilra, A., & Halassa, M. M. (2018). Thalamic regulation of switching between cortical representations enables cognitive flexibility. *Nat Neurosci*, *21*(12), 1753-1763. https://doi.org/10.1038/s41593-018-0269-z

Robbins, T. W., Weinberger, D., Taylor, J. G., Morris, R. G., Roberts, A. C., Robbins, T. W., & Weiskrantz, L. (1996). Dissociating executive functions of the prefrontal cortex. *Philosophical Transactions of the Royal Society of London. Series B: Biological Sciences*, *351*(1346), 1463-1471. https://doi.org/doi:10.1098/rstb.1996.0131

Sadaghiani, S., & D'Esposito, M. (2014). Functional Characterization of the Cingulo-Opercular Network in the Maintenance of Tonic Alertness. *Cerebral Cortex*, *25*(9), 2763-2773. https://doi.org/10.1093/cercor/bhu072

Sadaghiani, S., Scheeringa, R., Lehongre, K., Morillon, B., Giraud, A.-L., D'Esposito, M., & Kleinschmidt, A. (2012). Alpha-Band Phase Synchrony Is Related to Activity in the Fronto-Parietal Adaptive Control Network. *The Journal of Neuroscience*, *32*(41), 14305-14310. https://doi.org/10.1523/jneurosci.1358-12.2012

Sakai, K. (2008). Task set and prefrontal cortex. *Annu. Rev. Neurosci.*, *31*(1), 219-245.

Sattelberger, J., Haque, H., Juvonen, J. J., Siebenhühner, F., Palva, J. M., & Palva, S. (2024). Local and interareal alpha and low-beta band oscillation dynamics underlie the bilateral field advantage in visual working memory. *Cerebral Cortex*, *34*(11). https://doi.org/10.1093/cercor/bhae448

Sauseng, P., Griesmayr, B., Freunberger, R., & Klimesch, W. (2010). Control mechanisms in working memory: a possible function of EEG theta oscillations. *Neuroscience & Biobehavioral Reviews*, *34*(7), 1015-1022.

Sauseng, P., Klimesch, W., Doppelmayr, M., Pecherstorfer, T., Freunberger, R., & Hanslmayr, S. (2005). EEG alpha synchronization and functional coupling during top-down processing in a working memory task. *Human Brain Mapping*, *26*(2), 148-155. https://doi.org/10.1002/hbm.20150

Sauseng, P., Klimesch, W., Freunberger, R., Pecherstorfer, T., Hanslmayr, S., & Doppelmayr, M. (2006). Relevance of EEG alpha and theta oscillations during task switching. *Experimental Brain Research*, *170*(3), 295-301. https://doi.org/10.1007/s00221-005-0211-y

Sauseng, P., & Liesefeld, H. R. (2020). Cognitive Control: Brain Oscillations Coordinate Human Working Memory. *Current Biology*, *30*(9), R405-R407. https://doi.org/https://doi.org/10.1016/j.cub.2020.02.067

Singer, W. (1999). Neuronal synchrony: a versatile code for the definition of relations? *Neuron*, *24*(1), 49-65.

Spooner, R. K., Wiesman, A. I., Proskovec, A. L., Heinrichs-Graham, E., & Wilson, T. W. (2020). Prefrontal theta modulates sensorimotor gamma networks during the reorienting of attention. *Human Brain Mapping*, *41*(2), 520-529. https://doi.org/https://doi.org/10.1002/hbm.24819

Tsuchida, A., & Fellows, L. K. (2013). Are core component processes of executive function dissociable within the frontal lobes? Evidence from humans with focal prefrontal damage. *Cortex*, *49*(7), 1790-1800. https://doi.org/https://doi.org/10.1016/j.cortex.2012.10.014

Turi, Z., Mittner, M., Lehr, A., Bürger, H., Antal, A., & Paulus, W. (2020). θ-γ cross-frequency transcranial alternating current stimulation over the trough impairs cognitive control. *eneuro*, *7*(5).

van Driel, J., Ridderinkhof, K. R., & Cohen, M. X. (2012). Not all errors are alike: theta and alpha EEG dynamics relate to differences in error-processing dynamics. *Journal of Neuroscience*, *32*(47), 16795-16806.

Vandierendonck, A. (2017). A comparison of methods to combine speed and accuracy measures of performance: A rejoinder on the binning procedure. *Behavior Research Methods*, *49*(2), 653-673. https://doi.org/10.3758/s13428-016-0721-5

Vandierendonck, A., Liefooghe, B., & Verbruggen, F. (2010). Task switching: interplay of reconfiguration and interference control. *Psychological Bulletin*, *136*(4), 601.

Verguts, T. (2017). Binding by Random Bursts: A Computational Model of Cognitive Control. *Journal of Cognitive Neuroscience*, *29*(6), 1103-1118. https://doi.org/10.1162/jocn_a_01117

Verstraeten, E., & Cluydts, R. (2002). Attentional switching-related human EEG alpha oscillations. *NeuroReport*, *13*(5), 681-684. https://journals.lww.com/neuroreport/fulltext/2002/04160/attentional_switching_related_human_eeg_alpha.29.aspx

von Stein, A., & Sarnthein, J. (2000). Different frequencies for different scales of cortical integration: from local gamma to long range alpha/theta synchronization. *Int J Psychophysiol*, *38*(3), 301-313. https://doi.org/10.1016/s0167-8760(00)00172-0

Voytek, B., Kayser, A. S., Badre, D., Fegen, D., Chang, E. F., Crone, N. E., Parvizi, J., Knight, R. T., & D'esposito, M. (2015). Oscillatory dynamics coordinating human frontal networks in support of goal maintenance. *Nature Neuroscience*, *18*(9), 1318-1324.

Wolff, M., & Halassa, M. M. (2024). The mediodorsal thalamus in executive control. *Neuron*, *112*(6), 893-908. https://doi.org/10.1016/j.neuron.2024.01.002

Zanto, T. P., Rubens, M. T., Thangavel, A., & Gazzaley, A. (2011). Causal role of the prefrontal cortex in top-down modulation of visual processing and working memory. *Nature Neuroscience*, *14*(5), 656-661. https://doi.org/10.1038/nn.2773

Zhang, X., Mukherjee, A., Halassa, M. M., & Chen, Z. S. (2025). Mediodorsal thalamus regulates task uncertainty to enable cognitive flexibility. *Nature Communications*, *16*(1), 2640. https://doi.org/10.1038/s41467-025-58011-1